ELSEVIER

Ceramics International 25 (1999) 389–394

CERAMICS INTERNATIONAL

Investigation of grain boundary sliding during superplastic deformation of a fine-grained alumina by atomic force microscopy

L. Clarisse, A. Bataille, Y. Pennec, J. Crampon, R. Duclos*

Laboratoire de Structure et Propriétés de l'Etat Solide, URA CNRS 234, Bât. C6, Université des Sciences et Technologies de Lille, 59655 Villeneuve d'Ascq Cedex, France

Received 4 February 1998; accepted 27 March 1998

Abstract

The contribution of grain boundary sliding to total strain has been investigated in a superplastically deformed fine-grained alumina by atomic force microscopy in contact mode. The analysis of the surface relief and of its change with strain allowed us to determine the vertical component of grain boundary sliding as a function of strain up to 16%. Grain boundary sliding has been thus estimated to contribute to about 70% of total strain. This value is compared with results published on alumina ceramics or superplastic metallic alloys. The reliability and the limitation of the method are also discussed.

Keywords: D. Alumina; Superplasticity; Grain boundary sliding; Atomic force microscopy

1. Introduction

Deformation of polycrystalline ceramics is largely dependent on grain boundary sliding. This relative motion of two adjacent grains is a step required either to maintain the material cohesion and to avoid the formation of grain boundary cracks [1], as in the case of pure diffusion mechanisms, or to produce the main part of deformation as this is observed in the superplastic behaviour of fine-grained ceramics. In this last case the real contribution of grain boundary sliding to total strain can be large but its determination is not easy. Methods that are well adapted to materials with a large grain size, such as (i) marker lines on the surface specimen and measurement of offsets after deformation [1–6] or (ii) measurement of step height perpendicular to specimen surface by interferometric methods [7–9] or conventional surface analysis [10] for instance, are not easily transposable to ceramics with a grain size as fine as 1 μm or less. Besides the indirect method that consists in measuring the grain shape anisotropy after deformation [11–15] generally overestimates this contribution because grains tend to keep an equiaxed shape due to boundary mobility [10] and surface energy minimization.

In this paper an attempt to estimate the contribution of grain boundary sliding to total strain in a superplastically deformed fine-grained alumina is made by using atomic force microscopy (AFM). In contact mode, the microscope behaves as a high resolution surface analyser and provides a surface analysis with a high accuracy that allowed us to observe the changes in relief with increasing strain. The results deduced from this analysis are compared to those obtained from grain shape changes.

2. Experimental

The alumina used in this study was a commercial alumina (HR8 Criceram, Jarrie, France) doped with 500 ppm MgO and 4000 ppm ZrO_2. A disk of this material was fully densified by hot-pressing at 1400°C under a pressure of 30 MPa. The initial average grain size was 0.98 ± 0.03 μm. From the disk a specimen ($7 \times 3 \times 3$ mm) with the compression axis parallel to the pressing direction was cut and one of the lateral faces was first diamond polished and then thermally etched to reveal grain boundaries. This surface was examined by AFM (Digital Instruments) in contact mode before creep and after compressive strains ε of 4, 8, 12 and 16%,

* Corresponding author.

0272-8842/99/$20.00
PII: S0272-8842(98)00044-3

respectively, performed at 1350°C under a stress of 50 MPa. In each case six 10×10 μm areas (512×512 points) at least were analysed and determination of the grain boundary sliding component perpendicular to the specimen surface (the *v* component in Fig. 1) was made on three of these areas, the total number of measurements being about 450 for each strain (in such conditions the spatial resolution was better than 20 nm in the horizontal *xy* plane and better than 0.5 nm in the perpendicular *z* direction). The boundaries selected for this analysis were those intercepted by nine lines, parallel to the compression axis and equidistant (1.1 μm). For each selected boundary the perpendicular component *v* was estimated by measuring at the grain boundary place the vertical offset (later on "offset" or "component *v*" will be used interchangeably with the same meaning) between the planes that fitted surfaces of adjacent grains with the best agreement (Fig. 2).

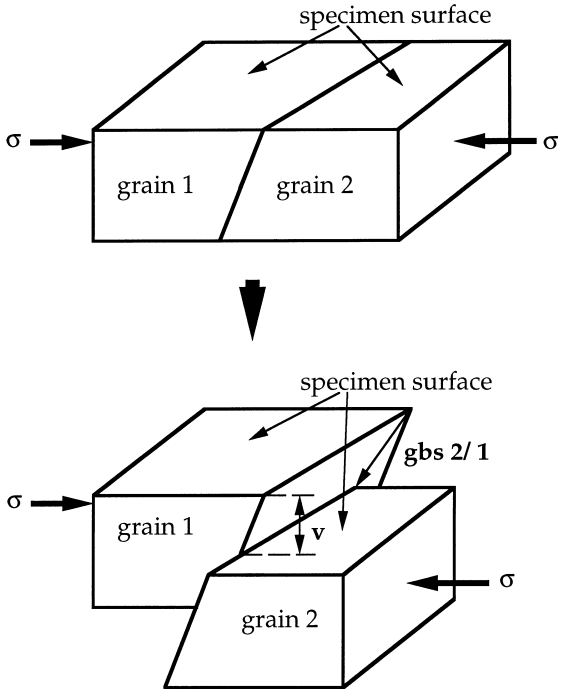

Fig. 1. Definition of the vertical component *v* of the grain boundary sliding.

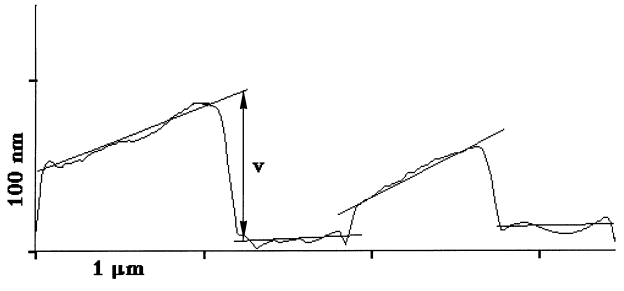

Fig. 2. Example showing the procedure used to determine the vertical component *v*.

3. Results

Fig. 3 shows the specimen surface (a) in the uncrept state and (b) after strains of 4%, (c) 8%, (d) 12% and (e) 16%, respectively. The grey colour scale accounts for the surface height, white for the highest surface elements and black for the lowest ones. From these micrographs and from Fig. 4, that presents a surface plot after a 16% strain, the effect of grain boundary sliding is highly visible: surface relief is more and more important when strain increases. According to procedure described in part 2 the vertical offsets have been determined for each analysed area and then arranged by ascending value, to allow easier comparisons. Fig. 5 presents the various curves; for each strain the three curves are very similar. They clearly indicate that the offset values are increasing with strain. From these curves the distribution functions of the offset values have been deduced. They are shown in Fig. 6 as a plot of the fraction of offsets in the ranges 0–25, 25–50, 50–75 nm, etc. The increment value of 25 nm is wide enough to take into account in each range an adequate number of measurements and avoids too much scatter. While about 80% of the offset values in the uncrept state are in the range 0–25 nm, after a strain of 16%, half of the values are higher than 50 nm, values larger than 200 nm being recorded. This corresponds to a flattening and a broadening of the distribution curve with increasing strain, a behaviour accounting for an increase in grain boundary sliding.

From the whole range of offset values, the mean vertical component $< v >$ of the grain boundary sliding has been calculated for each analysed 10×10 μm area. The result is reported in Fig. 7 as a plot of $< v >$ vs strain. The second series of data in this figure represents the surface roughness Ra, directly determined by the microscope. A correlation exists between these two kinds of results supporting the idea that, indirectly, roughness measurements would be able to account for grain boundary sliding. However the direct use of these measurements is not simple because they take into consideration numerous information like grain surface shape, boundary depth, cavities, etc., that can depend on surface preparation. Except at zero strain, the experimental values $< v >$ can be fitted by a straight line whose slope is 2.92 ± 0.3 nm/%. Note that during creep tests, the average grain size was very stable (1.02 μm after the strain of 16%).

From determination of the grain aspect ratio (here defined as the mean average grain size in a direction parallel to the compression axis over that in the perpendicular direction), an attempt to estimate the contribution of intragranular deformation to total strain was made. Fig. 8 presents this quantity vs strain. Due to the weak evolution of the aspect ratio and to the experimental scatter it is difficult to draw a reliable conclusion, except that intragranular deformation seems very small.

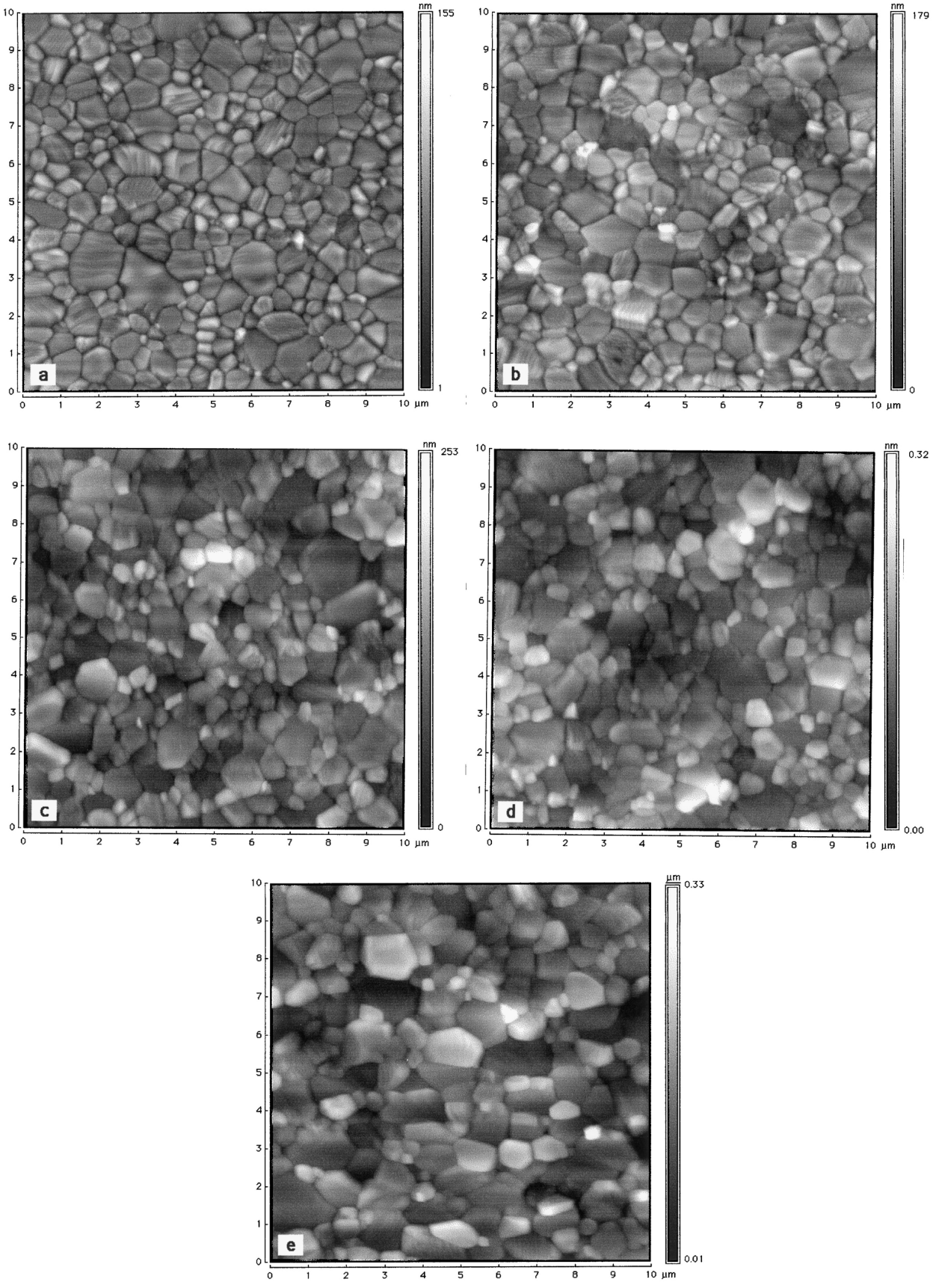

Fig. 3. AFM micrographs showing the change in surface relief with increasing strain: (a) 0%; (b) 4%; (c) 8%; (d) 12%; (e) 16%.

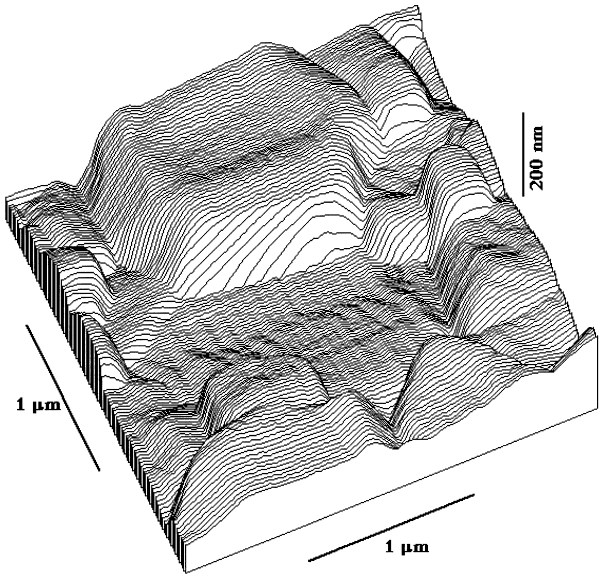

Fig. 4. Surface plot showing the effect of grain boundary sliding after a 16% strain [central part of Fig. 3(e)].

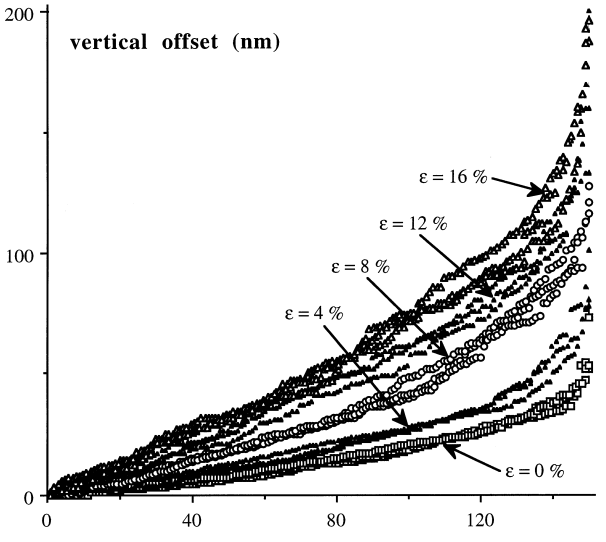

Fig. 5. Plot by ascending order of the vertical offsets v for the different analysed areas. Note the good reproductibility of the three curves for a given strain. 150 boundaries have been considered in each case.

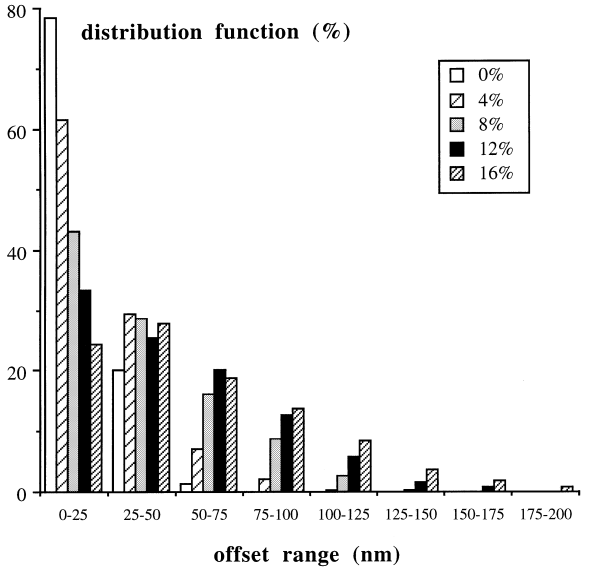

Fig. 6. Distribution functions of the offset value vs offset range.

4. Discussion

4.1. Reliability and limitation of the method

In this work the atomic force microscope was used as a high resolution surface analyser. The knowledge of the three coordinates x, y and z of each point of the specimen surface should allow determination of the change in the z component across any grain boundary. However due to thermal etching of boundaries and to tip shape (the tip is a Si_3N_4 pyramid with a 4×4 μm basis and 3 μm high), grain edges do not appear very sharp but rather rounded and thereby the real offset between two neighbour grains is partly screened; this is the reason why this offset was determined by comparing each grain surface to a plane (Fig. 2). Nevertheless this is not always easy when grain surfaces are curved. This disadvantage can be minimized by careful polishing and with thermal etching conditions that avoids too rapid surface diffusion to preserve surfaces as flat as possible. This means also that deformation conditions must prevent any change in the grain surface shape, as produced by rapid surface diffusion or by oxidation in the case of non-oxide materials. This is a restriction that must be taken into account to avoid surface artefacts. Beyond this remark, it seems that the procedure is reproducible enough, a good agreement between the three curves obtained at each strain exists (Fig. 5), to claim that this analysis method is reliable in the present case. Yet from curves in Figs. 5 and 7, it can be ascertained that the experimental scatter slightly increases with strain. This can be explained by the facts that (i) deformation is not really homogeneous in the whole specimen, (ii) not only grains suffer translation but also rotation (that is difficult to take into consideration) whose amplitude increases with strain and (iii) due to grain boundary sliding it is also possible that small grains leave the specimen surface, modifying its topography.

These observations suggest that the results obtained by this method would be more difficult to analyse at higher strains on such fine grained materials. They are consistent with conclusions drawn by Shariat et al. [4]. However, Lin et al. [5] showed that information obtained at low elongation (up to 50%) in a Zn–22% Al eutectoid alloy were not very different from those obtained at higher elongations (200%). Under these

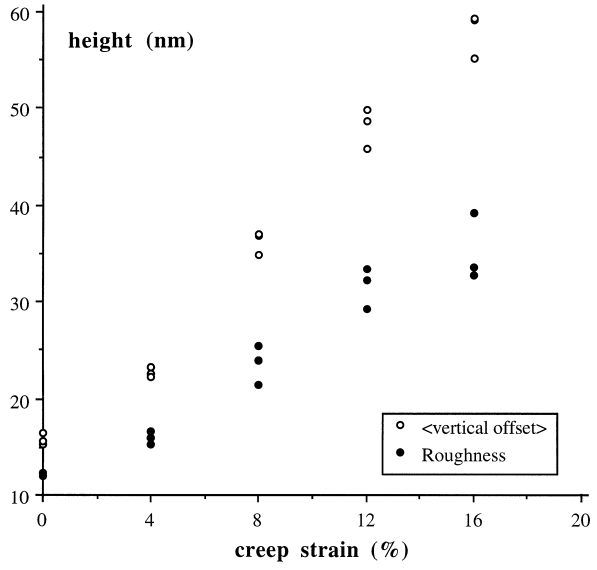

Fig. 7. Average offset value and roughness against strain for each investigated 10×10 μm area.

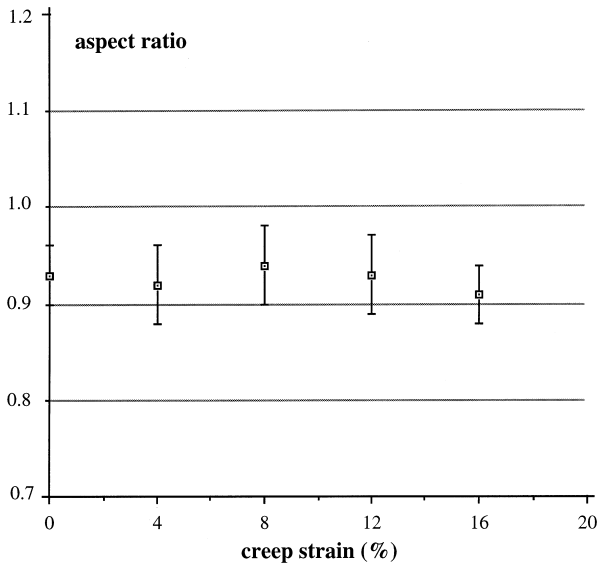

Fig. 8. Dependence of the grain aspect ratio upon strain.

conditions one can believe that our results can be generalized to higher strains.

4.2. Determination of the strain resulting from grain boundary sliding

Fig. 7 presents the evolution of $< v >$, the average vertical component of the grain boundary sliding, as a function of strain ε and shows that the specimen surface is not strictly flat in the uncrept state, i.e. that $< v > \neq 0$ for $\varepsilon = 0$. Under these conditions the calculation of the strain ε_{gbs} resulting from grain boundary sliding cannot be deduced according to the relation initially proposed by Langdon [1]:

$$\varepsilon_{gbs} = \phi n_l < v > \quad (1)$$

where n_l is the number of grains per unit length and ϕ is a numerical factor equal to 1.4 for an annealed surface. From Eq. (1) the contribution of grain boundary sliding to total strain ε_{tot} is defined as $\gamma = \varepsilon_{gbs}/\varepsilon_{tot}$, i.e. presently:

$$\gamma = 1.4 n_l [< v(\varepsilon) > /\varepsilon] \quad (2)$$

To account for the above observation at $\varepsilon = 0$, Eq. (2) has been modified and the relative strain γ has been estimated according to relation:

$$\gamma = \varepsilon_{gbs}/\varepsilon_{tot} = 1.4 n_l [d < v(e) > /d\varepsilon] \quad (3)$$

where the term in brakets is the slope of the line that fits the experimental data in Fig. 7 after a strain of 4%. The increase in strain from 0 to 4%, that does not entail a similar increase in offset, is probably due to a transient during which preexisting offsets can be either amplified or, on the contrary, reduced due to the boundary orientation relative to that of the compression axis. According to the slope (2.92 ± 0.3 nm/%) and to the value of n_l (1.74 grain/μm) a relative strain $\gamma = 0.71 \pm 0.08$ is obtained. Due to the above remarks concerning the change in grain shape anisotropy with strain, it is difficult to compare the results obtained by the two methods. One can simply assess in the present case that the change in grain shape anisotropy cannot account for a contribution of intragranular strain to total strain of 30%.

4.3. Comparison with the literature

The value of the sliding contribution of 71% shows that grain boundary sliding is preponderant in this kind of material, a consistent conclusion owing to the very fine grain size that allowed us the observation of superplastic behaviour [16].

This value is consistent with those already published concerning alumina polycrystals. Cannon and Sherby [10] determined a contribution of grain boundary sliding to total strain of 58 and 44% for two aluminas, a medium-grained one (14 to 30 μm) and a coarse-grained one (65 μm), respectively. It is known that intragranular strain is larger in coarse-grained materials than in fine-grained ones. This explains a lower sliding contribution in this study. More recently Chokshi [6], by measuring the offset in markers lines, obtained a grain boundary sliding contribution of 70% for an alumina with a grain size of 9.5 μm, a value comparable to ours.

Our value is also in good agreement with measurements of grain boundary sliding in the superplastic region II for metallic alloys. For these materials, sliding

contributions of 50 to 70% of the total strain have been reported in the region of maximum superplasticity [3,5], while this contribution decreased to values of about 20% in the less superplastic regions I and III.

5. Conclusions

This study showed that atomic force microscopy is a suitable method to evaluate grain boundary sliding and its contribution to total strain in fine-grained ceramics. In the case of an alumina material with a mean grain size of 1 μm, for which a superplastic behaviour has been already identified [16], the contribution of grain boundary sliding to total strain yielded an average value of 71%. This result is very encouraging and suggests the use of this technique to other fine-grained ceramics, not only for the determination of the grain boundary sliding, but also for the dependence of this sliding with the kind of interface in two phase materials for example. In this case AFM images must be coupled with SEM observations to be certain of the phase distribution, image contrast being not dependent on the phase chemistry in the different ceramics materials we have tested (alumina/zirconia, spinel/zirconia).

References

[1] T.G. Langdon, Grain boundary deformation processes, in: R.C. Bradt, R.E. Tressler (Eds.), Deformation of Ceramic Materials, Plenum Press, New York, 1975, pp. 101–126.
[2] T.G. Langdon, Effect of surface configuration on grain boundary sliding, Metall. Trans. 3 (1972) 797–801.
[3] R.B. Vastava, T.G. Langdon, An investigation of intercrystalline and interphase boundary sliding in the superplastic Pb-62% Sn eutectic, Acta Metall. 27 (1979) 251–257.
[4] P. Shariat, R.B. Vastava, T.G. Langdon, An evaluation of the roles of intercrystalline and interphase boundary sliding in two-phase superplastic alloys, Acta Metall. 30 (1982) 285–296.
[5] Z.R. Lin, A.H. Chokshi, T.G. Langdon, An investigation of grain boundary sliding in superplasticity at high elongations, J. Mater. Sci. 23 (1988) 2712–2722.
[6] A.H. Chokshi, An evaluation of the grain-boundary sliding contribution to creep deformation in polycrystalline alumina, J. Mater. Sci. 25 (1990) 3221–3228.
[7] R.C. Gifkins, T.G. Langdon, On the question of low temperature sliding at grain boundaries, J. Inst. Metals 93 (1964) 347–352.
[8] T.G. Langdon, Grain-boundary sliding during creep of MgO, J. Amer. Ceram. Soc. 58 (1975) 92–93.
[9] T. Chandra, J.J. Jonas, D.M.R. Taplin, Grain-boundary sliding and intergranular cavitation during superplastic deformation of α/β brass, J. Mater. Sci. 13 (1978) 2380–2384.
[10] W.R. Cannon, O.D. Sherby, Creep behavior and grain-boundary sliding in polycrystalline Al_2O_3, J. Amer. Ceram. Soc. 60 (1977) 44–47.
[11] F. Wakai, H. Kato, Superplasticity of TZP/Al_2O_3 composite, Adv. Ceram. Mater. 3 (1988) 71–76.
[12] J.H. Hensler, G.V. Cullen, Grain shape change during creep in magnesium oxide, J. Amer. Ceram. Soc. 50 (1967) 584–585.
[13] A.G. Crouch, High-temperature deformation of polycrystalline Fe_2O_3, J. Amer. Ceram. Soc. 55 (1972) 558–563.
[14] M. Tokar, Compressive creep and hot hardness of U-Pu carbides, J. Amer. Ceram. Soc. 56 (1973) 173–177.
[15] R. Martinez, R. Duclos, J. Crampon, Structural evolution of a 20% ZrO_2/Al_2O_3 ceramic composite during superplastic deformation, Scripta Metall. Mater. 24 (1990) 1979–1984.
[16] L. Clarisse, R. Baddi, A. Bataille, J. Crampon, R. Duclos, J. Vicens, Superplastic deformation mechanisms during creep of alumina-zirconia composites, Acta Mater. 45 (1997) 3843–3853.